Neuron, Volume 55
Supplemental Data

Action-related properties shape object representations in the ventral stream

Bradford Z. Mahon, Shawn C. Milleville, Gioia A.L. Negri, Raffaella I. Rumiati, Alfonso Caramazza, Alex Martin

Supplemental Online Experimental Procedures

Ratings of experimental stimuli for motor relevant properties

Instructions for ‘predictability of object identity from movement” (n = 16) (see Figure 1A): “Suppose you were playing charades, such that one person had to identify an object/thing based on how another person mimed various actions that might be associated with that object/thing. You are asked to rate, for the following objects/things, how difficult it would be to play that game with these items. (1 = very easy; 7 = very difficult/impossible).” There was a graded difference across the nonliving object types in the degree to which the identities of the objects were predictable from the movements associated with those objects (‘tools’ (mean = 2.3; Standard Error of the Mean (SEM) = .12) > arbitrarily manipulated objects (mean = 3.6; SEM = .18) > nonmanipulable objects (mean = 5.0; SEM = .25; Linear contrast analysis: $F = 165.4$, $p < .001$; $\eta^2 = .92$).

Instructions for ‘centrality of motor movement’ (n = 16) (see Figure 1B): “How central is the pattern of movement(s) associated with the use of this object/thing in determining its function? (1 = not central at all; 7 = very central).” The motor movements associated with the use of ‘tools’ were more central in determining their function (mean = 5.1, SEM = .25) than arbitrarily manipulated objects ($p < .001$) (mean = 3.1; SEM = .15) and nonmanipulable objects ($p < .001$) (mean = 3.5; SEM = .13). Arbitrarily manipulated objects and nonmanipulable objects did not differ on this dimension ($p = .03$) at the corrected alpha level.

Instructions for ‘familiarity in manipulating objects’ ($n = 10$) (see Figure 1C): “Rate each object based on how frequently you interact with the object/thing with your hands. (1 = no experience interacting with the object/thing; 7 = frequently interact with the object/thing).” ‘Tools’ (mean = 4.6; SEM = .30) and arbitrarily manipulated objects (mean = 4.6; SEM = .16) were equivalent with regard to participants’ familiarity interacting with the objects ($p = .93$). Participants had more experience interacting with both ‘tools’ and arbitrarily manipulated objects than with nonmanipulable objects (both $ps < .001$).

Participants had 10 seconds to make each response, which was entered on a keyboard. The stimuli were presented in a different random order for all subjects. Each subject saw one exemplar of each item. The four exemplars of each item were counterbalanced across subjects. Paired-t-tests were used to compare the mean ratings within subjects across the nonliving object types; an alpha level of 1.5% (corrected for multiple comparisons) was used.

Analysis of similarity in visual shape within stimulus types

The similarity in visual shape within each stimulus type was assessed computationally using the algorithm described in Belongie et al. (2002). This algorithm samples 100 arbitrary points along the contour of an image *a*, and then solves for the correspondence between every sampled point in *a* and a corresponding set of points in image *b*. The amount of ‘work’ necessary to align image *a* with image *b* is then computed (this is plotted on the y axes of Figure 1D and Supplemental Figure S5). We calculated the similarity between every image within every stimulus type and every other image within that stimulus type (80 x 79 data points). We then calculated the average similarity (arithmetic mean) across the 79 data points for every image within a stimulus type. Figure 1D plots for each stimulus type, the distribution of similarity among items within that stimulus type.

In order to assess the sensitivity of this analysis, we also calculated the average similarity of a given image (e.g., exemplar 1 of the item 'elephant') to the other three exemplars of the corresponding item (i.e., the other three exemplars of 'elephant'). Separately, we calculated the similarity between the same image and the other items within the stimulus type (i.e., exemplar 1 of 'elephant' versus all other animal images, excluding the other exemplars of 'elephant'). Supplemental Figure S5 is a graphical representation of the results of this analysis. An ANOVA, collapsing across the factor Stimulus Type, showed that there was greater similarity in visual shape between different exemplars of the same items, than between different items ($F = 277.6$, $p < .001$). There was an interaction between this main effect and the factor Stimulus Type ($F = 14.6$, $p < .001$). Post-hoc analyses demonstrated that the difference between 'between-item' and 'between-exemplar' similarity was greater for all nonliving stimulus types compared to animals, as well as for nonmanipulable objects and arbitrarily manipulated objects compared to 'tools' (all ps $< .05$, Bonferroni corrected). There was no difference between nonmanipulable objects and arbitrarily manipulated objects ($p > .05$). Collectively, these analyses of visual shape similarity demonstrate that while (1) there was sensitivity to observe effects of visual shape similarity for each of the four stimulus types (Figure S5),

2) the overall similarity in visual shape within the stimulus types (Figure 1D) cannot account for the pattern of RS effects observed in the medial fusiform gyri.

Psycholinguistic variables

The stimulus types were matched on lexical frequency ($F < 1$) and concept familiarity ($F < 1$) but differed on number of phonemes ($p < .02$). Follow up t-tests (unpaired, two-tailed) showed that 'tools' had fewer phonemes than nonmanipulable objects ($p < .005$) and arbitrarily manipulated objects ($p < .005$) (all other ps $\geq .1$).

Naming latencies

Naming latencies were obtained from 14 right-handed participants (Native English Speakers) who did not take part in the fMRI study. Analyses of response times with two repeated factors, Stimulus Type (with four levels: animals, 'tools', arbitrarily manipulated objects, nonmanipulable) and Repetition (with two levels: novel, repeated) showed a main effect of Stimulus Type ($p < .001$) a main effect of repetition ($p < .003$) and a reliable interaction ($p < .001$). The interaction was due to relatively more behavioral priming for nonmanipulable objects than for animals. Importantly, (see text) there was reliable behavioral priming for all stimulus types (animals: $p = .052$; 'tools': $p < .001$; arbitrarily manipulated objects: $p < .001$; nonmanipulable: $p < .001$). Collapsing across the factor Repetition, there were no differences between animals (mean = 855ms) and arbitrarily manipulated objects (mean = 850ms) ($F<1$), animals and 'tools' (mean = 864ms) ($p = .28$), or arbitrarily manipulated objects and 'tools' ($p = .105$). Naming latencies for nonmanipulable objects (mean = 897ms) were slower than for all other stimulus types (all ps $< .001$).

Stimulus presentation and timing

For both the imaging and behavioral portions of the study, Presentation Software (Neurobehavioral Systems, Inc.) was used to present the stimuli and maintain precise timing of the presentation of the stimuli as well as synchronization with MRI. The 640 stimulus trials were presented over 5 separate runs. Each run contained 128 trial events on average. A trial consisted of a 500ms presentation of the stimulus, immediately followed by a 1500ms fixation cross, for a total trial time of 2000ms. Stimulus presentation was jittered and the optimum sequence program OptSeq determined the randomized sequence of events and jittered null trials. Each null trial consisted of 1000ms of a fixation cross. The overall timing of null trials over the five runs was equivalent to the overall timing of any given stimulus type collapsed across repetition. A variable inter-trial interval (ITI) was used, with variable ITIs of 0, 1, 2, or 3 seconds. The mean time across the experiment between stimulus presentations was 2007.8 ms.

Functional Connectivity Analysis

To perform the connectivity analysis, the voxel with the peak t-value within the left medial fusiform gyrus defined by the comparison of All Nonliving versus animals (see Figure 2) was selected as the seed voxel. The neuronal strength of the seed voxel was estimated by deconvolving the seed voxel time series with a Gamma hemodynamic response function (HRF) using MATLAB 7.1. The neuronal level interaction was the product of the stimulus time series and the neuronal seed time series, and the interaction at the neuronal level was convolved with a Gamma HRF to represent the time series at the hemodynamic level (see Gitelman et al., 2003 for more information). Two interaction HRFs were created for each stimulus condition, one for novel trials and one for repeated trials. In order to look at priming effects, the interaction HRF for repeated conditions was subtracted from the novel conditions at each time point of the time series. The functional connectivity analysis was performed through multiple regression analyses of the subject's functional data with time series created for the seed voxel, the stimulus priming condition, and the interaction between the seed and stimulus priming. To perform group connectivity analysis, the interaction correlation coefficients were converted to Gaussian following Fisher's Z transformation formula for each individual subject. A one-sample t-test against 0 using the individual Z scores was performed for the group analysis (see Figure 8 and Supplemental Table S3).

Neuropsychological Study

Because the objective of the object naming task was to determine whether the patients were able to recognize the object at a basic level, patients were allowed to self-correct after making phonological errors or dysfluencies. Patients with severe language impairments were administered a multiple choice task in place of the naming task. In the multiple choice task, three color photographs were presented simultaneously, and the experimenter said aloud the name of the target picture. Distractor pictures were semantically related (e.g., target: pen; distractors: eraser, scissors).

Performance on the object use task was scored with a three point scale (2 if correct on the first attempt; 1 if recognizable but with difficulty or after an initially incorrect attempt, and 0 if unable to perform the action in a recognizable manner).[1]

The lesion analyses reported in the manuscript were performed after transforming patients' performance profiles into discrete values (0 impaired; 1 not impaired).

---

[1] For details of the patient testing, see G.A.L.N., R.I.R., A. Z., M.U., B.Z.M., and A.C., unpublished data. For copies of the manuscript describing the behavioral testing of the patients, email the corresponding author (mahon@fas.harvard.edu).

However, the same pattern of lesion overlap was observed when the analyses were carried out using continuous data (t-scores, logistic regression; MRIcro) to predict lesioned voxels.

The group of 42 patients were also administered an object decision task (VOSP) in which the patients are asked to judge whether a presented object represents a real or an unreal object (VSOP; Warrington and James, 1991). The performance of patients was classified as impaired or not impaired using the published norms for age-specific mean performance, and the statistical tools described in Crawford and Garthwaite (2006). For the analysis described in Figure 7, patients were separated according to whether their lesions involved the parietal cortex. This was done using the Brodmann area template in MRIcro (http://www.sph.sc.edu/comd/rorden/mricro.html) by an author (G.A.L.N) who was, at the time, blind to the purpose of the analysis.

References

Belongie, S., Malik, J., and Puzicha, J. (2002). Shape matching and object recognition using shape contexts. Transactions on pattern analysis and machine intelligence, 24, 509-522

Gitelman, D.R., Penny, W.D., Ashburner, J., and Friston, K.J. (2003). Modeling regional and psychophysiologic interactions in fMRI: the importance of hemodynamic deconvolution. NeuroImage, 200-207

Supplemental Figure S1

All histograms represent mean (+SEM) BOLD responses averaged across all voxels in the region for the contrast displayed; all images are at y = -42. **A** Regions in the medial fusiform gyrus more active for 'tools' than animals (blue). **B** Regions more active for arbitrarily manipulated objects than animals (blue). When the right hemisphere region was defined by arbitrarily manipulated objects versus animals at a more strict statistical threshold ($p < .001$, reducing the region to 4,208mm3) RS was observed for both arbitrarily manipulated objects ($p < .039$) and 'tools' ($p < .0002$). **C** Regions more active for nonmanipulable objects than animals (blue). The relative difference in the size of these object-responsive regions remained (**D**) when bilateral medial fusiform regions were defined using only novel trials for each of the nonliving object types compared to animals. Thus, these relative size differences were not due to differential RS effects.

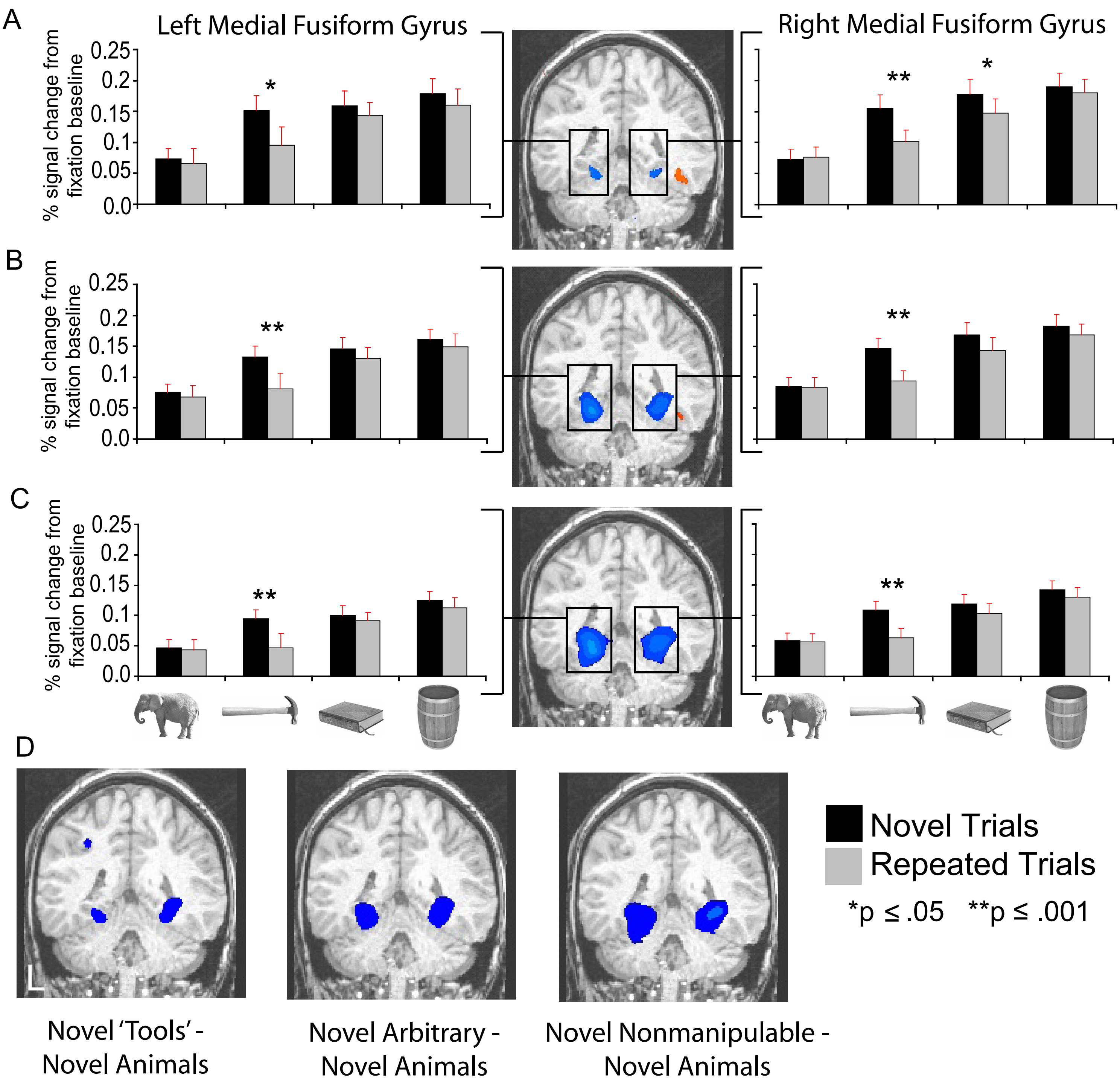

Supplemental Figure S2

RS restricted to ‘tools’ (blue) was observed in left ventral premotor cortex (left axial view at z = 24) and in bilateral anterior IPS (aIPS) (right axial view at z = 34). RS restricted to arbitrarily manipulated objects was observed in left dorsal premotor cortex and right ventral and dorsal premotor cortex. In caudal IPS (cIPS), RS was observed for both ‘tools’ and arbitrarily manipulated objects in the right hemisphere.

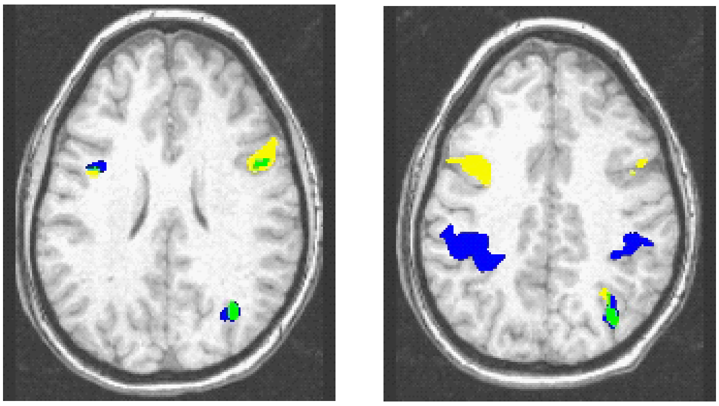

‘Tool’ RS only

Arbitrary RS only

‘Tool’ and arbitrary RS only

Supplemental Figure S3

The purpose of this analysis was to confirm, using a different approach, that patients with lesions in the left middle temporal gyrus and/or the left inferior parietal lobule, were in fact driving the correlation reported in Figure 7A. In the analysis summarized below, patients were separated into those who were impaired on either (or both) object identification or object use, and those whose performance was spared. This was done separately for those patients with lesions involving the parietal cortex (Panel A) and those with lesions not involving the parietal cortex (Panel B). The red-white color bar indicates z scores for lesion overlap in patients who were impaired for object use or object identification. The blue-green color bar indicates z scores for lesion overlap in patients who were not impaired for either object use or object identification.
This analysis confirms that patients who were impaired for either (or both) object use and object identification showed lesion overlap in the critical regions of the left middle temporal gyrus and the left inferior parietal lobule.

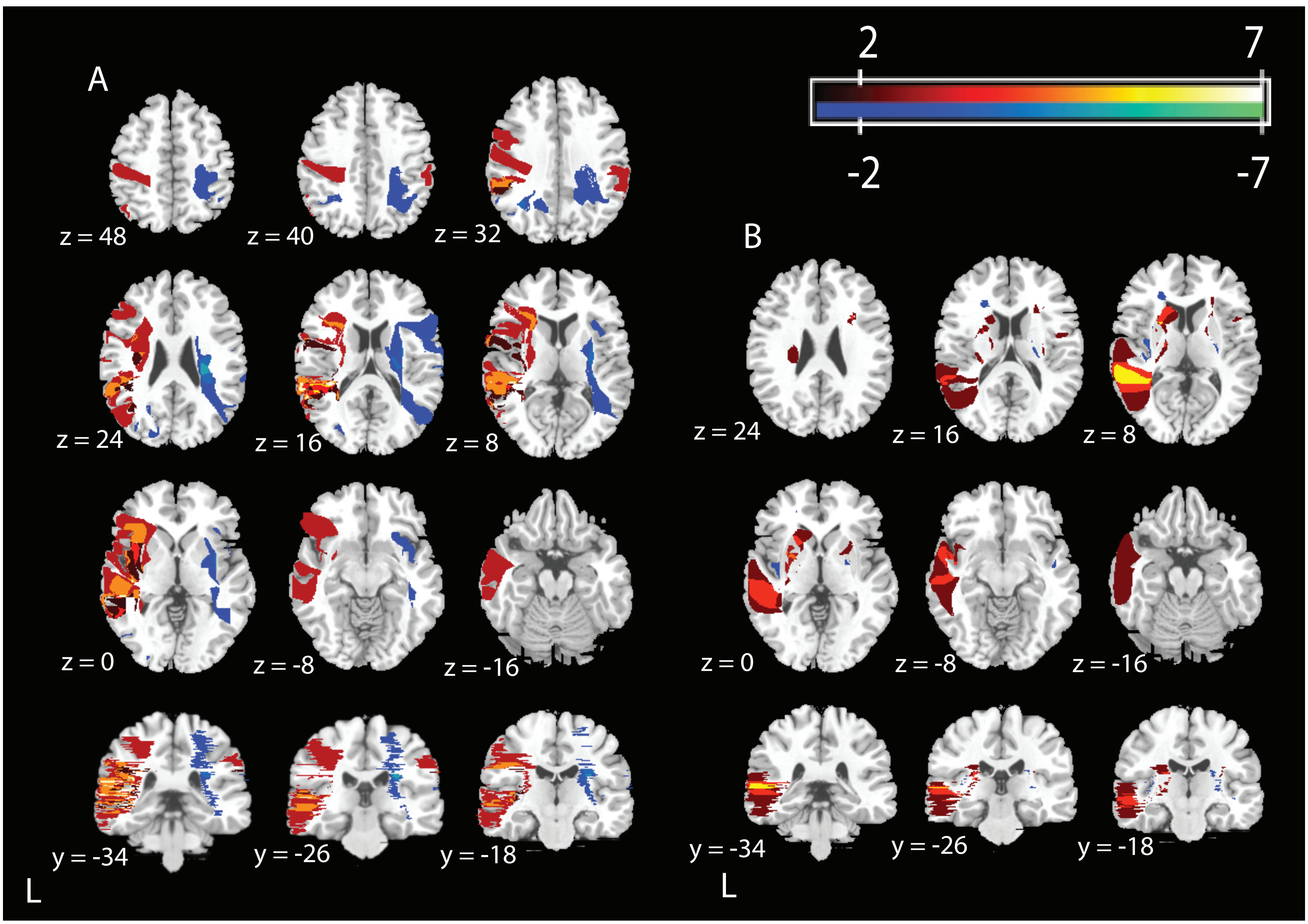

Supplemental Figure S4

Supplemental Figure S4

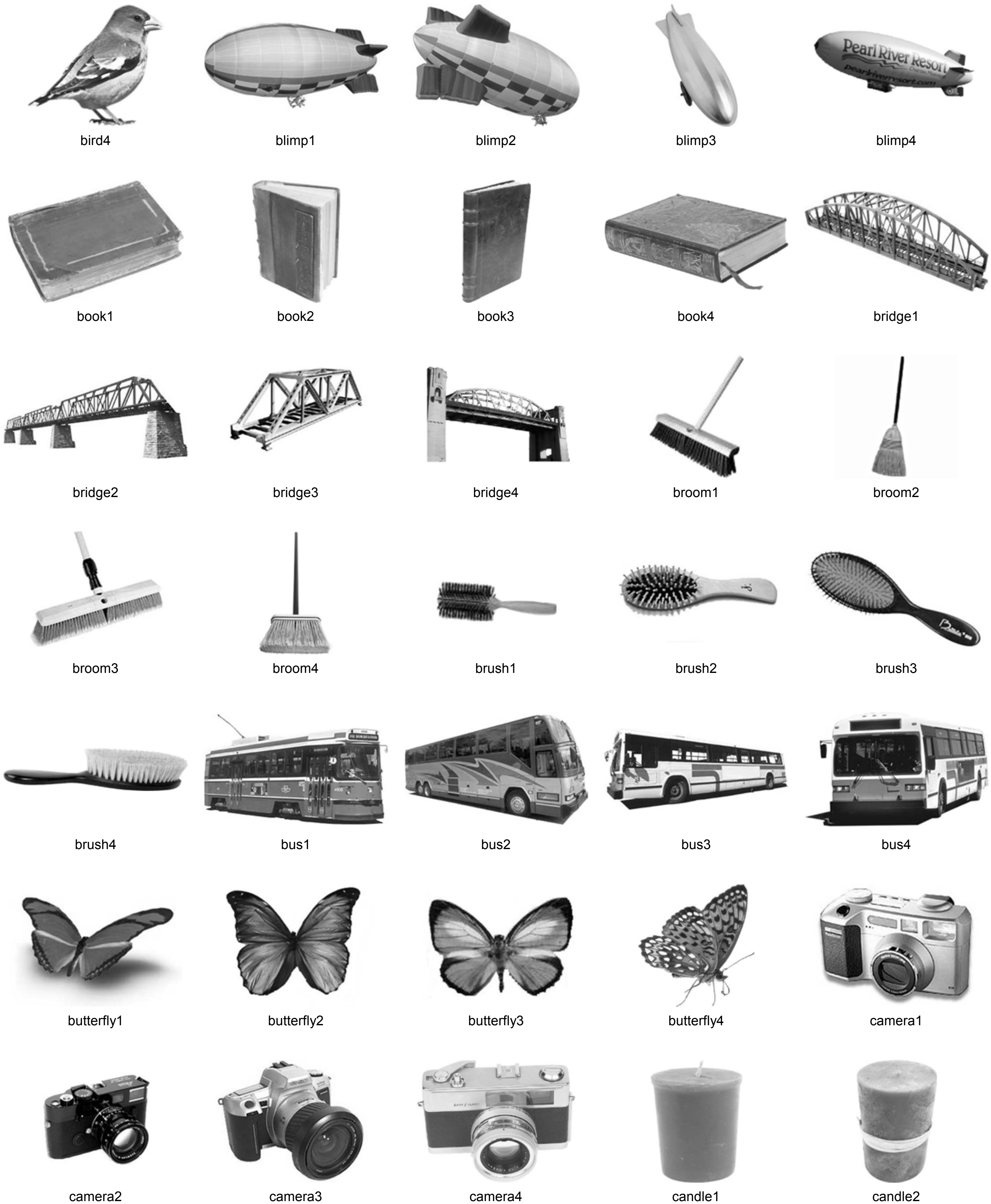

Supplemental Figure S4

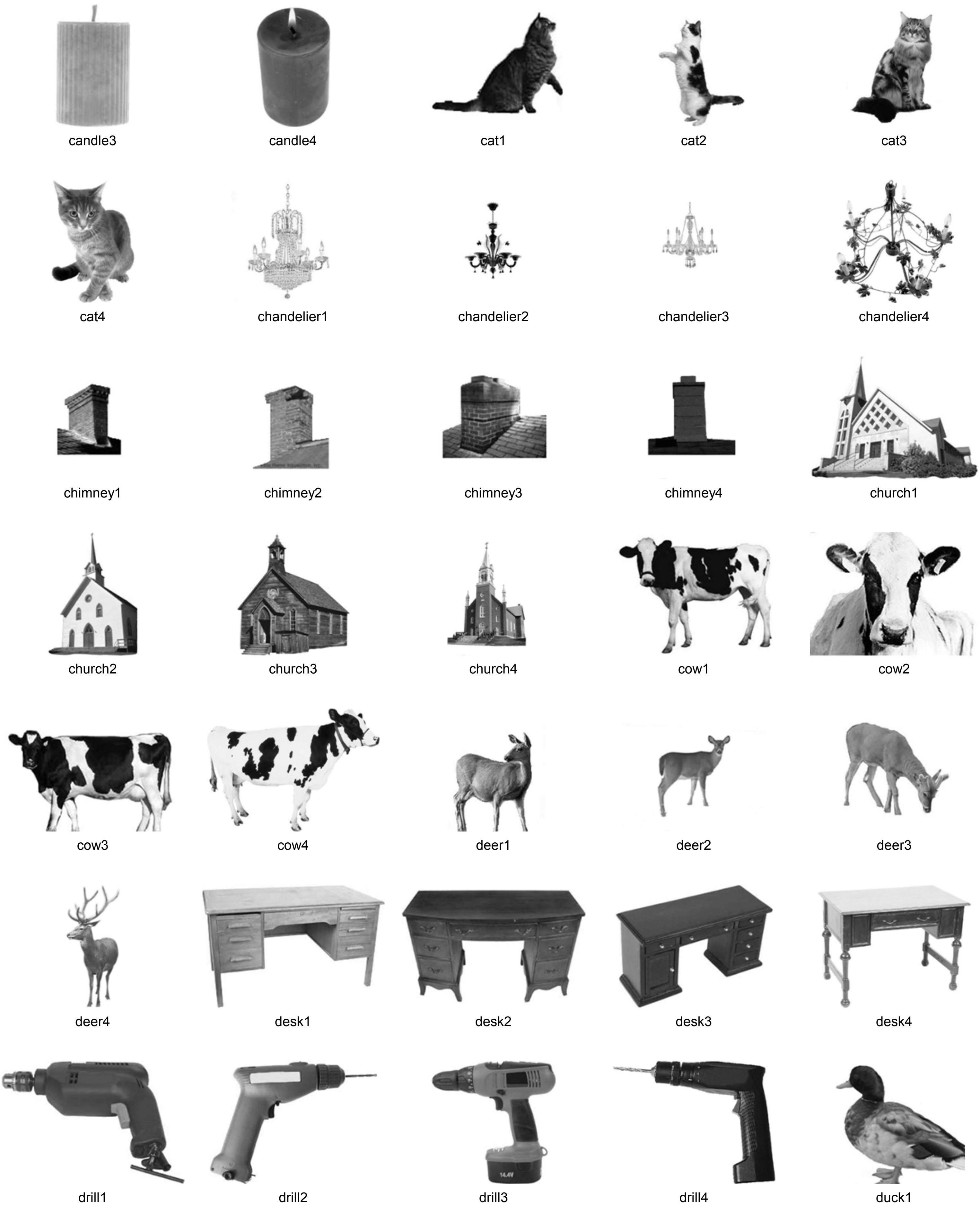

Supplemental Figure S4


duck2


duck3


duck4


easel1


easel2


easel3


easel4


elephant1


elephant2


elephant3

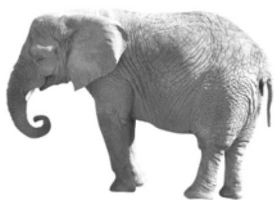
elephant4


envelope1


envelope2


envelope3


envelope4


fan1


fan2


fan3


fan4


fence1


fence2


fence3


fence4


file1


file2


file3


file4


fork1


fork2


fork3


fork4


glass1


glass2


glass3


glass4


hammer1
hammer2
hammer3
hammer4
hammock1
hammock2
hammock3
hammock4
horse1
horse2
horse3
horse4
iron1
iron2
iron3
iron4
kettle1
kettle2
kettle3
kettle4
knife1
knife2
knife3
knife4
lantern1
lantern2
lantern3
lantern4
lobster1
lobster2
lobster3
lobster4
matches1
matches2
matches3

Supplemental Figure S4

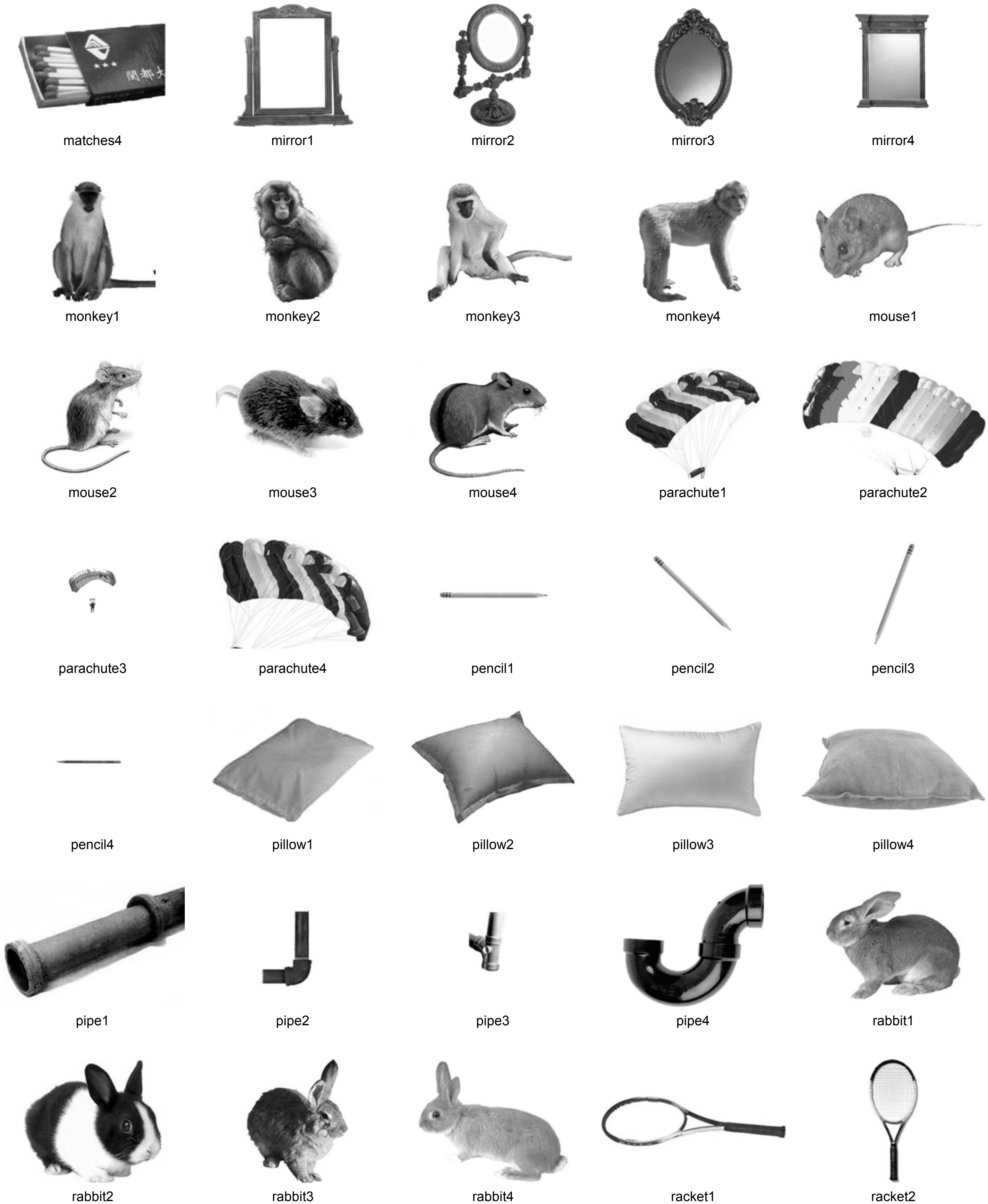

Supplemental Figure S4

Supplemental Figure S4

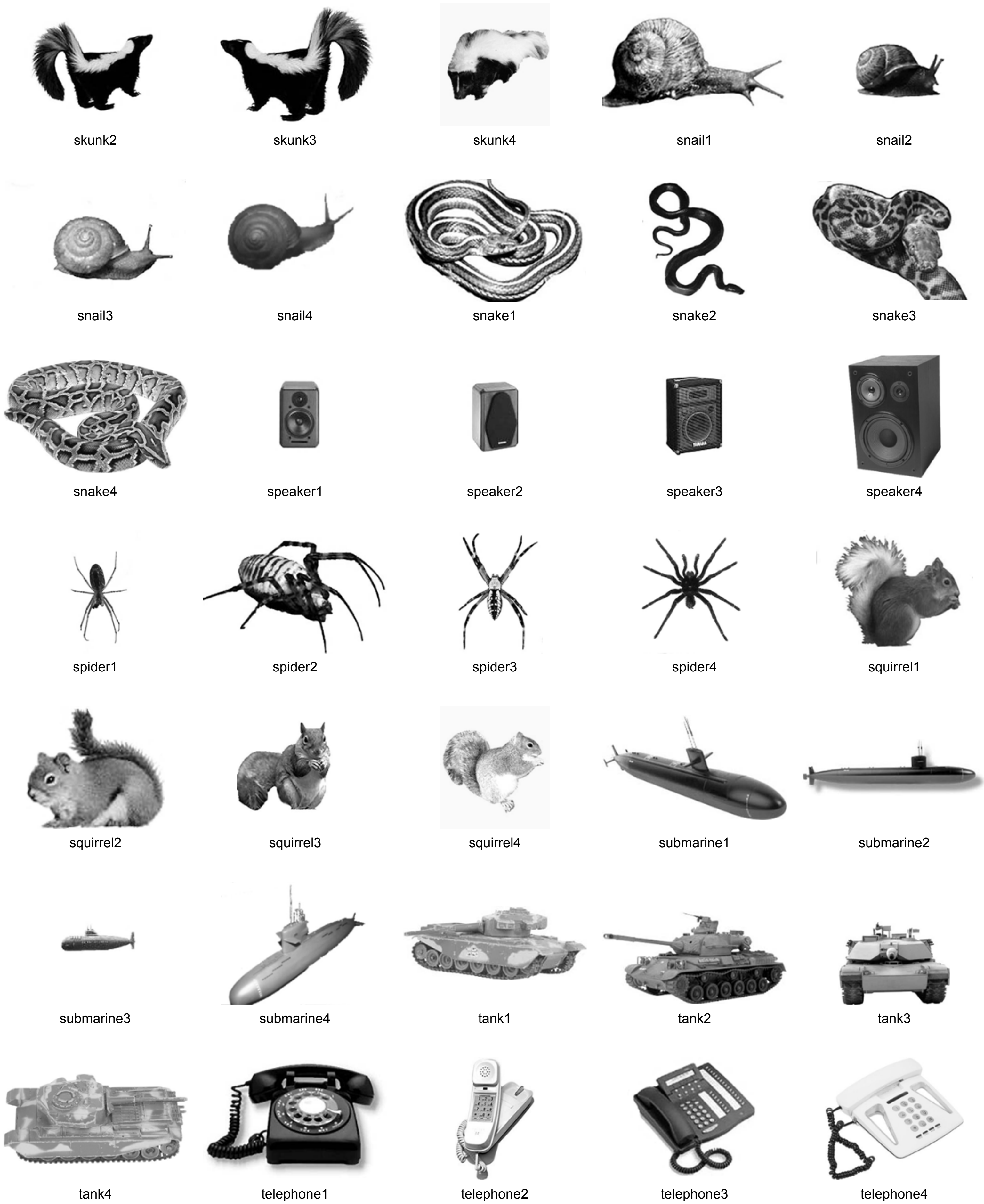

Supplemental Figure S4

Supplemental Figure S4

watch4

wrench1

wrench2

wrench3

wrench4

Supplemental Figure S5

This graph demonstrates that the analysis of visual shape similarity had sensitivity to detect differences in visual shape similarity within each stimulus type. See Supplemental Online Experimental Procedures for discussion. Box plot represents medians ± inter-quartile ranges (IQRs). Outliers (circles) and extreme values (stars) are defined as values between 1.5 - 3 IQRs, and greater than 3 IQRs, respectively, from the tops and bottoms of the boxes.

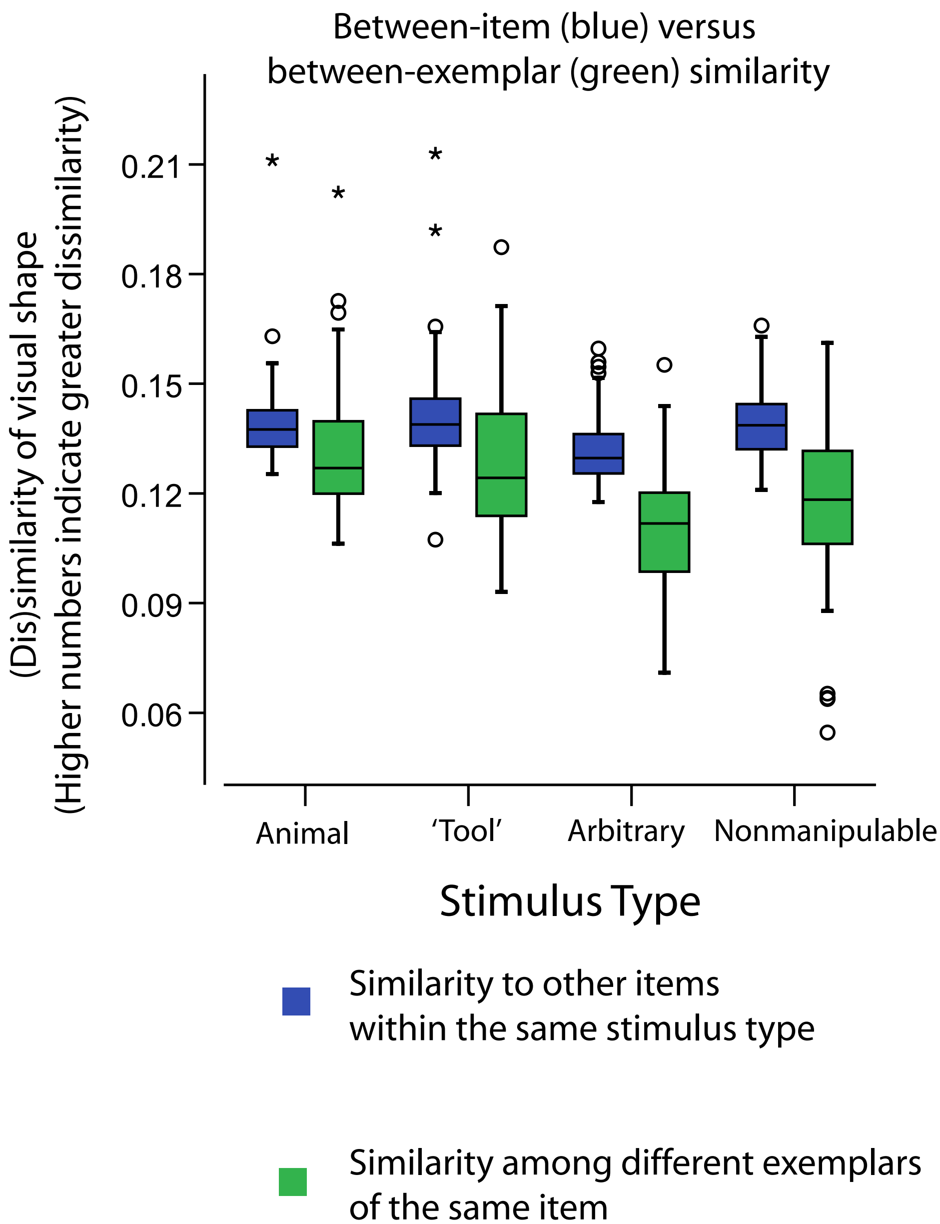

Supplemental Table S1a: Locations and RS profiles by stimulus type for regions showing enhanced activity for ‘tools’ versus animals

	‘Tools’ vs. Animals					
	Location	Size	Animal RS	Tool RS	Arbitrary RS	Nonmanipulable RS
L. Medial Fusiform	-23, -50, -9	1,929mm^3	F < 1	**p < .002**	F < 1	p = .271
R. Medial Fusiform	21, -40, -14	783mm^3	F < 1	**p < .0002**	**p < .029**	F < 1
L. Middle Temporal Gyrus	-49, -61, -7	1,156mm^3	F < 1	**p < .024**	p = .151	F < 1
L. Dorsal Occipital	-31, -82, 20	1,520mm^3	F < 1	**p < .006**	p = .309	F < 1
R. Dorsal Occipital	34, -78, 16	952mm^3	F < 1	p =. 101	p = .198	F < 1
L. cIPS .	-16, -67, 44	3,416mm^3	F < 1	**p = .052**	F < 1	p*= .248
R. cIPS	24, -64, 36	223mm^3	F < 1	**p < .018**	**p < .031**	F < 1
L. Inferior Parietal	-57, -27, 34	1,600mm^3	F < 1	**p < .020**	F < 1	F < 1
L. Premotor	-49, 3, 28	50mm^3	F < 1	p = .065	**p < .025**	p* = .090

* = value on novel < value on repeated

Supplemental Table S1b: Locations and RS profiles by stimulus type for regions showing enhanced activity for arbitrarily manipulated objects versus animals

Arbitrarily manipulated objects vs. Animals						
	Location	Size	Animal RS	Tool RS	Arbitrary RS	Nonmanipulable RS
L. Medial Fusiform	-24. -48, -7	7,820mm^3	F < 1	**p < .001**	F < 1	F < 1
R. Medial Fusiform	28, -41, -10	7,493mm^3	F < 1	**p < .0005**	p = .076	F < 1
L. Middle Temporal Gyrus	-46, -57, -4	410mm^3	F < 1	**p < .009**	p = .205	p = .222
L. Dorsal Occipital	-30, -85, 20	5,444mm^3	F < 1	**p < .006**	p = .250	F < 1
R. Dorsal Occipital	37, -80, 18	3,737mm^3	F < 1	**p < .047**	p = .086	F < 1
L. cIPS	-18, -68, 29	773mm^3	F < 1	**p < .023**	p = .073	F < 1
R. cIPS	26, -69, 37	1,159mm^3	F < 1	**p < .007**	**p < .026**	F < 1

Supplemental Table S1c: Locations and RS profiles by stimulus type for regions showing enhanced activity for nonmanipulable objects versus animals

Nonmanipulable objects vs. Animals						
	Location	Size	Animal RS	Tool RS	Arbitrary RS	Nonmanipulable RS
L. Medial Fusiform	-24, -47, -7	12,373mm^3	F < 1	**p < .001**	F < 1	F < 1
R. Medial Fusiform	28, -38, -10	13,121mm^3	F < 1	**p < .0008**	p = .226	F < 1
L. Dorsal Occipital	-29, -86, 18	7617mm^3	F < 1	**p < .008**	p = .237	F < 1
R. Dorsal Occipital	35, -80, 18	8,090mm^3	F < 1	**p < .040**	p = .063	F < 1
L. cIPS	-19, -62, 36	1,930mm^3	F < 1	**p < .040**	p = .109	p* = .279
R. cIPS	20, -80, 48	4,937mm^3	F < 1	**p < .016**	p = .093	F < 1

* = value on novel < value on repeated

Supplemental Table S2

Full correlation matrix for all stimulus types comparing the rank ordered BOLD response by subjects in the left medial fusiform gyrus and the left inferior parietal lobule (see Figure 5B for details). As can be seen (bolded numbers), there was a reliable correlation only for 'tools' between BOLD repsonses in the two regions.

			Nonmanipulable		Arbitrary		'Tool'		Animal	
			L. Inf. Parietal	L. Medial Fusiform	L. Inf. Parietal	L. Medial Fusiform	L. Inf. Parietal	L. Medial Fusiform	L. Inf. Parietal	L. Medial Fusiform
Animal	L. Medial Fusiform	Spearman r	-0.35	**0.841**	-0.184	**0.831**	0.243	**0.868**	-0.208	-
		p(2-tailed)	0.168	**0.000**	0.48	**0.000**	0.348	**0.000**	0.422	-
	L. Inf. Parietal	Spearman r	**0.605**	-0.23	**0.676**	-0.292	0.319	-0.203	-	
		p(2-tailed)	**0.01**	0.374	**0.003**	0.256	0.213	0.434	-	
'Tool'	L. Medial Fusiform	Spearman r	-0.338	**0.775**	-0.108	**0.924**	**0.549**	-		
		p(2-tailed)	0.184	**0.000**	0.68	**0.000**	**0.022**	-		
	L. Inf. Parietal	Spearman r	0.265	0.311	0.461	0.377	-			
		p(2-tailed)	0.305	0.224	0.063	0.135	-			
Arbitrary	L. Medial Fusiform	Spearman r	-0.336	**0.757**	-0.13	-				
		p(2-tailed)	0.188	**0.000**	0.619	-				
	L. Inf. Parietal	Spearman r	**0.578**	-0.277	-					
		p(2-tailed)	**0.015**	0.282	-					
Nonmanipulable	L. Medial Fusiform	Spearman r	-0.096	-						
		p(2-tailed)	0.715	-						
	L. Inf. Parietal	Spearman r	-							
		p(2-tailed)	-							

Supplemental Table S3. Regions identified in the functional connectivity analysis showing RS restricted to 'tools.' Bolded rows indicate the regions discussed in the text and in Figure 8. The numbers within each column labeled by stimulus type indicate the t-value of the RS effect. t-value = 2.120, p = 0.05; t-value = 2.919, p = 0.01, t-value = 3.992, p = 0.001

TT coordinates			Stimulus Type				Anatomical Description
X	Y	Z	Animal	'Tool'	Arbitrary	NonManipulable	
-15	-47	-7	0.22	3.91	-0.87	1.63	fusiform/lingual gyrus
-46	-40	-23	-1.51	4.12	-1.47	-1.33	left cerebellum
-47	-56	-30	-0.45	3.92	-1.10	0.81	left cerebellum
-43	-41	50	1.40	4.27	-2.02	-1.02	left inferior parietal lobule
-30	-38	47	2.58	3.64	-0.12	-0.46	left inferior parietal lobule
-51	**-34**	**36**	**1.02**	**3.26**	**0.26**	**-0.08**	**left inferior parietal lobule**
-59	-32	41	0.90	3.36	-0.34	-0.67	left inferior parietal lobule
-64	**-47**	**-12**	**-0.83**	**3.78**	**0.74**	**-0.37**	**left lateral temporal cortex**
-18	-64	7	-0.26	3.39	-2.28	1.92	left lingual gyrus
-14	-35	35	0.47	4.33	-0.95	-0.26	left middle cingulum
-7	-35	71	1.57	3.80	-0.78	0.78	left precuneus
-45	-39	15	1.41	4.06	-1.34	0.55	left superior temporal cortex